

# Wind Turbine Condition Monitoring Based on Assembled Multidimensional Membership Functions Using Fuzzy Inference System

Fuming Qu, Jinhai Liu, *Member, IEEE*, Hongfei Zhu and Dong Zang

**Abstract**—Condition monitoring (CM) has been playing an important role in the operation and maintenance of industrial equipment. However, the changeable environments where some equipment, such as wind turbines (WTs) are installed, have put a negative effect on CM. To deal with this problem, this paper proposes a CM method of WTs based on assembled multidimensional membership functions (MFs) using fuzzy inference system (FIS). First, multidimensional MFs, which are formed by fusing environment factor into conventional MFs, are proposed to reduce the negative effect from changeable environments. Second, the input data are properly divided into segments and the segments are classified into four types to distinguish the effects of different data on CM. Different weights are assigned to each segment and the corresponding membership of each segment is calculated separately. Then, these memberships are assembled for fuzzy inference. Finally, based on the assembled multidimensional MFs, a new CM architecture is established. Four groups of experiments were carried out to evaluate the proposed method with the data collected from a wind farm in northern China. The experiments results show that the proposed method can not only detect anomalies at an early stage but also effectively decrease the false alarms and missing detections.

**Index Terms**—wind turbine, condition monitoring, multidimensional membership function, assembled memberships, fuzzy inference system.

## I. INTRODUCTION

**A**S a new type of clean energy, wind power has gained a remarkable growth in the past few years [1]. However, with the increasing installation of wind turbines (WTs), the high operation and maintenance (O&M) cost [2] is becoming an important issue. Many researches have been explored to address this problem, among which, condition monitoring (CM) is one of the key technologies. CM is a process of monitoring the operating parameters of a physical system. From the change(s) in the parameter(s), possible failure(s) in the system can be diagnosed and prognosed [3]. A robust CM system, which can predict faults before they occur, could lead to remarkable reduction in O&M [4]. Therefore, there have been increasing researches focusing on CM [5]–[7], making CM a major subject in the field of industrial informatics.

Fuming Qu was with the Collage of Information Science and Engineering, Northeastern University, Shenyang, 110819, China. Jinhai Liu was with State Key Laboratory of Synthetical Automation for Process Industries, the Collage of Information Science and Engineering, Northeastern University, Shenyang, 110819, China. Hongfei Zhu and Dong Zang were with the Collage of Information Science and Engineering, Northeastern University, Shenyang, 110819, China. e-mail: steve\_qufm@126.com, liujinhai@mail.neu.edu.cn, steve\_zuhf@126.com and zangdong723@126.com

CM is usually applied to detecting anomalies, diagnosing and prognosing faults [8]. CM studies in WT fields consist of the following categories in accordance with different monitored data types [9]: vibration analysis [10], acoustic emission analysis [11], lubrication analysis [12], supervisory control and data acquisition (SCADA) data analysis [13], etc. Among these monitored data, SCADA data provide hundreds of condition variables such as temperatures, wind parameters, energy conversion parameters, which are suitable for data-driven methods [14] and big data analysis [15]. Therefore, studies on SCADA data have gained a momentum of rapid growth in recent years [16]–[18].

The CM methods based on SCADA data can be divided into many categories, represented by the following methods.

**Classification-based methods.** These methods attempt to find the relationship between independent monitored variables and predefined categories (such as “healthy”, “warning”, etc) [19]. In [20], an intelligent fault diagnosis method was proposed to automatically identify health conditions of WT gearbox. In [21], a data-driven framework was presented to detect WT blade surface cracks.

**Regression-based methods.** These methods usually model normal behaviour of WT components and adopt regression approaches to predict the output for anomaly detection. In [22], a framework based on deep neural network was developed to monitor conditions of WT gearboxes and detect the impending faults. In [23], a CM method based on the nonlinear state estimate technique for a WT generator was presented.

**Fuzzy-based methods.** With the development of fuzzy theories [24], fuzzy methods, such as fuzzy inference system (FIS), are applied to monitoring conditions in many studies. In [25], a fault diagnosis method based on identified fuzzy models was proposed. In [26], a small-sample WT fault detection method with the synthetic fault data was presented. WT faults were detected using the generated fault data. In [27], a fuzzy synthetic model based on a real-time condition assessment method was developed. In [28], based on the fuzzy theory, a generalized anomaly detection model which integrated different data prediction models was proposed. In [29], a CM system of WTs using adaptive neuro-fuzzy interference systems was developed and many WT fault detection applications using FIS were presented in [30].

However, unlike other industrial equipment, WTs are exposed to harsh environments [31]. The changeable environments (such as wind speed, humidity, etc) have negatively affected the accuracy of CM methods, especially for the methods

based on FIS. That brings many drawbacks in the current FIS methods: (1) It is noticed that most current FIS approaches consider little about the changeable environment, which could result in the inaccuracy of CM. (2) Moreover, the changeable data in a day are also ignored in the conventional methods, which could result in the failure to detect the anomaly at an early stage.

Due to the above motivations, this paper proposes a CM method based on assembled multidimensional membership functions (MFs) using FIS. Unlike conventional MFs, multidimensional MFs are introduced to make the CM more flexible and adaptable. Also, the monitored data are properly divided into segments and classified into four types. Then, different membership weights are assigned to each segment, and multiple memberships are assembled for fuzzy inference. By doing so, the CM and anomaly detection of WTs can be more effective.

The contributions of this paper include:

(1) A novel multidimensional MF in WT condition monitoring is proposed to deal with the changeable environments, which are ignored by the conventional FIS methods.

(2) The assembled weighted memberships are proposed to elaborately process the changeable data, making the condition monitoring more flexible and adaptable.

(3) Based on the assembled multidimensional MFs, a new WT condition monitoring architecture is established, so that false alarms and missing detections are reduced.

The rest of this paper is organized as follows. Section II is the related work and problem descriptions. Section III presents the proposed method. Experiments are listed in Section IV. Section V summarizes the conclusion of the present work.

## II. RELATED WORK AND PROBLEM DESCRIPTIONS

The main process of the conventional CM method of WTs based on FIS can be divided into three phases as summarized in Fig. 1.

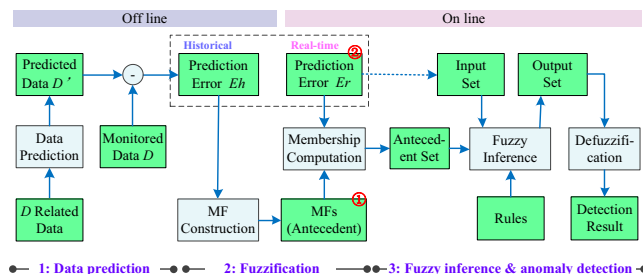


Fig. 1. Process of the conventional CM method.

Phase 1: Data prediction. Normally, prediction errors are used as the input data of FIS [29]. Prediction errors are calculated as follows: suppose  $D = [D_1, D_2, \dots, D_n]$  are the collected data, where  $D_i$  is the  $i$ th variable (such as active power, wind direction, etc). If  $D_s$  is the designated monitored variable, it is predicted by its related variables (the variables that are highly correlated with  $D_s$ ) as:

$$D'_s = f(D_C, D_H) \quad (1)$$

where  $D_C$  are the current related variables of  $D_s$  and  $D_H$  are the historical related variables of  $D_s$ .  $f$  is the data prediction method. The neural network (NN) method, which proves as an effective approach in predicting data [19], is adopted by many CM studies [32], [33]. Then, the prediction error can be obtained by (2).

$$E_s = D_s - D'_s \quad (2)$$

Phase 2: Fuzzification. In this phase, prediction errors (crisp data) are transformed to fuzzy set by MFs. First, MFs are established by fuzzy statistics method [28] using the historical off-line prediction error  $E_h$ . Then, the online prediction error  $E_r$  are processed by the established MFs. By doing so, the crisp data can be transformed to the fuzzy set (the antecedent set) as shown in Fig. 1. Meanwhile,  $E_r$  are also used as the singleton input set of the fuzzy inference.

Phase 3: Fuzzy inference and anomaly detection. Using the obtained fuzzy sets, fuzzy inference is applied to producing the fuzzy output in accordance with the rules. Rules are generally extracted by the prior knowledge and expert experiences. [30] lists many rules for CM of WTs, and the following is an example: “IF (spinner temp.==high) AND (nacelle temp.==ok) THEN (diagnosis: spinner temp. high) (root cause: sensor defect)”. Finally, anomalies can be detected based on FIS output.

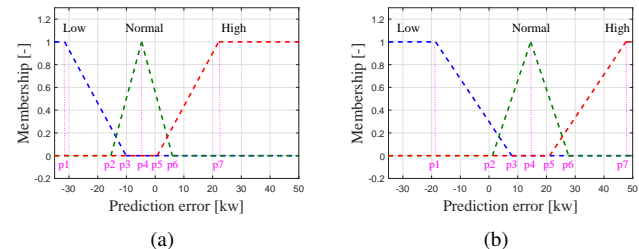


Fig. 2. MFs of prediction error (active power) under different wind speeds: (a)  $5\pm0.5$  m/s. (b)  $7\pm0.5$  m/s.

However, the conventional methods have the following two limitations.

First, conventional methods use only one single group of MFs in all environment conditions (marked with the red ① in Fig. 1). Unlike the FIS applied in stable environments, the FIS of WTs is negatively affected by changeable environments. Fig. 2 shows an example. It can be found that the MFs are quite different under different environment conditions (different wind speeds in this case).

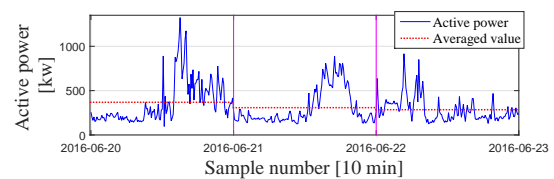


Fig. 3. Real data of the active power in three days.

Second, conventional methods use daily averaged data as the crisp input of fuzzification (marked with the red ② in Fig. 1), which can hardly tell data details. Fig. 3 shows an example.

In three consecutive days, the data (active power in this case) fluctuated drastically. In such case, the daily averaged data are not suitable for CM.

### III. THE PROPOSED METHOD

#### A. Multidimensional Membership Function

In this part, multidimensional MFs are proposed to reduce the negative effect from changeable environments on FIS.

In conventional methods, MFs are usually two dimensional. For example, the MF of term “low” in Fig. 2 has two dimensions (prediction error and membership), which can be expressed by Zadeh representation as:

$$\mu_l(x) = \int_{-\infty}^{p_1} \frac{\mu_{p_1}(x)}{x} + \int_{p_1}^{p_3} \frac{\mu_{p_1 p_3}(x)}{x} + \int_{p_3}^{\infty} \frac{\mu_{p_3}(x)}{x} \quad (3)$$

where  $x$  is the prediction error,  $\mu_l(x)$  is the membership and  $p_1$  is the critical point ( $p_1 \sim p_7$  in Fig. 2). All the MFs can be expressed as  $\varphi$  for short:

$$\mu(x) = \varphi(x|P = P_0) = \varphi(x) \quad (4)$$

where  $P$  is the vector of critical points (such as  $p_1 \sim p_7$  in Fig. 2) of the MFs. In the conventional methods,  $P$  is constant  $P_0$ .  $P_0$  can be obtained by fuzzy statistics method [28] using the historical data, and expressed as:

$$P_0 = fs(x) \quad (5)$$

where  $fs$  is the operator of fuzzy statistics.

However, from the experiments in Section II, it can be found that MFs are different if environment changes:

$$\varphi(x|P = P_1) \neq \varphi(x|P = P_2), \quad P_1 \neq P_2 \quad (6)$$

Therefore, enhanced MF  $\mu(x, e)$  is required to deal with both the input  $x$  and the environment  $e$  (such as wind speed), expressed as (7), so that the changeable environments can be properly handled.

$$\mu(x, e) = \Phi(x, e) \quad (7)$$

where  $\Phi(x, e)$  is the expression of the enhanced MF. However,  $\Phi(x, e)$  cannot be directly obtained by fuzzy statistics method. Inspired by the idea of fitting hyper-plane data in [34], this paper adopts the same idea to obtain  $\Phi(x, e)$  by fitting two-dimensional MFs (2D-MFs).

First, 2D-MFs in a specific environment condition are built. From (4) and (5), it can be deduced that: when using only the historical data in a certain environment  $e_i$ , the corresponding MFs can be obtained by the fuzzy statistics method as:

$$\mu(x|e = e_i) = \varphi(x|e = e_i) = \varphi(x|P = P_i) \quad (8)$$

where  $P_i$  can be calculated by:

$$P_i = fs(x|e = e_i) \quad (9)$$

Then, a series of 2D-MFs in different environment conditions can be obtained.  $\Phi(x, e)$  can be considered as an integration of all the 2D-MFs in different environment conditions. Therefore,  $\Phi(x, e)$  can be calculated by fitting all the obtained

2D-MFs:

$$\begin{aligned} \mu(x, e) &= \Phi(x, e) = fit[\varphi(x|P = P_1), \\ &\quad \varphi(x|P = P_2), \dots, \varphi(x|P = P_n)] \end{aligned} \quad (10)$$

where  $fit$  is the operation of data fitting. The cubic spline fitting method is effective and it is widely used in many industrial fields [35]. In this paper, the same method is adopted to fit 2D MFs.

By doing so, the new MF is obtained. Unlike the conventional 2D-MFs expressed in (4), the new MF has three dimensions (the input data dimension  $x$ , the environment dimension  $e$  and the membership dimension  $\mu$ ), so the new MF is a three dimensional MF (3D-MF). Fig. 4 shows an example of this process. First, conventional 2D-MFs are calculated by (8) and (9) in different environment conditions (different wind speeds in this case). Then, as shown in Fig. 4, all the 2D-MFs are fitted and combined as a 3D-MF. The 3D-MF has three dimensions: the input data (the prediction error), the environment data and the membership. Its membership is calculated not only by the input data but also by the environment data.

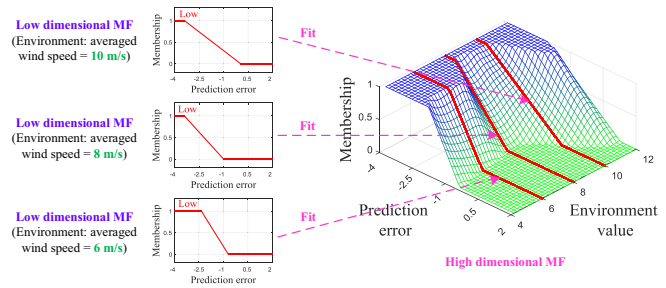


Fig. 4. Schematic of the fitting from 2D-MFs to 3D-MF.

In general, if there are more than one environment factors affecting the MFs, the  $n$ -dimensional MFs ( $n$ D-MFs) can also be calculated. Low dimensional MFs in a certain environment condition can be expressed as:

$$\mu(x|E = E_i) = \varphi(x|E = E_i) = \varphi(x|P = P_i) \quad (11)$$

where  $E$  is the vector of the environment variables,  $E = [e_1, e_2, \dots, e_n]$  and  $e_i$  is the  $i$ th environment variable (such as wind speed or humidity). Then,  $n$ D-MFs, like 3D-MFs, can be obtained by fitting all the low dimensional MFs together:

$$\begin{aligned} \mu(x, E) &= \Phi(x, E) = \Phi[(x, e_1), (x, e_2), \dots, (x, e_n)] \\ &= fit [\varphi(x|P = P_{11}), \dots, \varphi(x|P = P_{1m}), \\ &\quad \varphi(x|P = P_{21}), \dots, \varphi(x|P = P_{2m}), \\ &\quad \dots, \\ &\quad \varphi(x|P = P_{n1}), \dots, \varphi(x|P = P_{nm})] \end{aligned} \quad (12)$$

where  $P_{i,j}$  is parameter vector of the  $j$ th sub-condition under the  $i$ th environment condition. The multidimensional MFs can be also expressed by Zadeh representation as:

$$\mu(x, E) = \int_{E_1} \frac{\mu_{E_1}(x)}{x} + \int_{E_2} \frac{\mu_{E_2}(x)}{x} + \dots + \int_{E_n} \frac{\mu_{E_n}(x)}{x} \quad (13)$$

Fig. 5 shows an example of the 3D-MFs of the active power

in a WT.

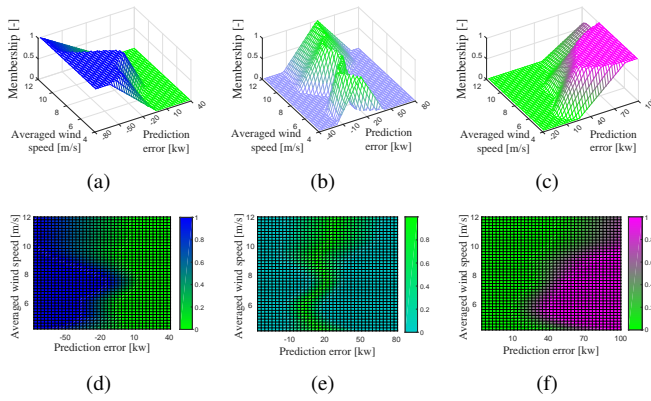


Fig. 5. An example of 3D-MFs of active power in a WT. 3D view: (a) Low. (b) Normal. (c) High. Colored 2D view: (d) Low. (e) Normal. (f) High.

Finally, the multidimensional MFs, which are more accurate than the conventional 2D-MFs, are used for CM of WTs.

### B. Assembled Memberships

In this subsection, assembled memberships are proposed to make the CM more flexible and adaptable. Fig. 6 shows the flowchart.

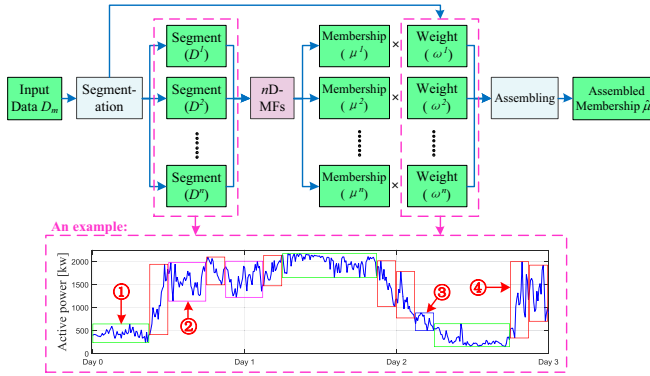


Fig. 6. Flowchart of data segmentation and membership calculation.

**1) Data segmentation:** First, in order to make a good use of the data those are effective for CM, the input data are divided into segments as illustrated in Fig 6. The input data  $D_m$  are divided by a predefined minimum length  $\gamma$ :

$$D_m = [D_\gamma^1, D_\gamma^2, \dots, D_\gamma^k] \quad (14)$$

where  $m$  is the length of  $D_m$ ,  $k$  is the segment number and  $m = \gamma \times k$ . Then, some adjacent segments are combined:

$$D_\eta^p = D_\gamma^{i+1} \cup D_\gamma^{i+2} \cup \dots \cup D_\gamma^{i+w} \quad (15)$$

if and only if  $\overline{|D_\gamma^{i+j} - D_\gamma^{i+j+1}|} < \tau$ ,  $j = 1, 2, \dots, w-1$ .  $\eta$  is the length of the combined segment  $D_\eta^p$ ,  $\eta = w \times \gamma$ ,  $\overline{D_\eta^p}$  is the averaged value of the data in  $D_\eta^p$  and  $\tau$  is the threshold. After the segmentation and combination, the input data can be divided into  $n$  ( $n \leq k$ ) segments of different lengths. Then, each segment is processed by the  $nD$ -MFs obtained in

Section III.A. Finally, memberships of all the segments can be obtained.

Fig. 7 shows an example of the membership calculation of a data segment: (1) Prediction errors of the segment are calculated and used as one dimension of the 3D-MF to determine the value of X-axis. (2) The corresponding environment data are used as another dimension to determine the value of Y-axis. Then, the membership of the third dimension (the value of Z-axis) can be finally calculated.

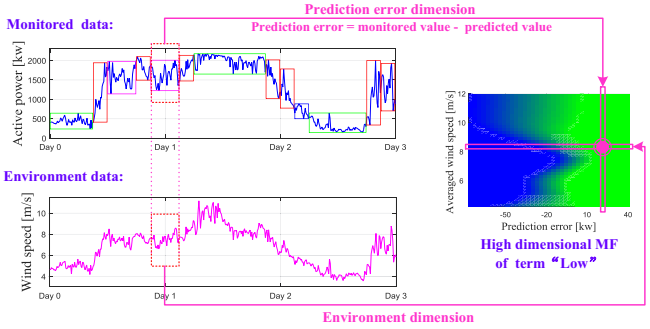


Fig. 7. Schematic of membership calculation of a segment by  $nD$ -MFs.

**2) Segment types:** Some of the divided segments are continuous and stable and such type of segments are suitable for CM, whereas some of the divided segments are not. Therefore, in this paper, four segment types are defined to distinguish the effect of segments on CM.

Suppose  $\eta$  is the length of a segment  $D_\eta^i$  and  $\gamma$  is the predefined minimum segment length.  $\sigma$  is the standard deviation of  $D_\eta^i$  and  $\bar{\sigma}$  is the averaged standard deviation of all the historical data under the same environment condition of  $D_\eta^i$ . Then, the segment types are defined as follows:

Type 1: Stable continuous data, defined by (16), illustrated as the red ① (the green box) in Fig. 6. This data segment is continuous and stable. It is highly effective for CM.

$$\eta > \gamma \quad \text{and} \quad \sigma \leq \bar{\sigma} \quad (16)$$

Type 2: Unstable continuous data, defined by (17), illustrated as the red ② (the pink box) in Fig. 6. This data segment is continuous, but its standard deviation is higher than normal.

$$\eta > \gamma \quad \text{and} \quad \sigma > \bar{\sigma} \quad (17)$$

Type 3: Stable discontinuous data, defined by (18), illustrated as the red ③ (the blue box) in Fig. 6. This data segment is stable, but with short length.

$$\eta = \gamma \quad \text{and} \quad \sigma \leq \bar{\sigma} \quad (18)$$

Type 4: Unstable discontinuous data, defined by (19), illustrated as the red ④ (the red box) in Fig. 6. This data segment is unstable and short. It is not suitable for CM.

$$\eta = \gamma \quad \text{and} \quad \sigma > \bar{\sigma} \quad (19)$$

**3) Segment weights:** In order to enhance the effect of high quality data and reduce the effect of poor quality data, different weights are defined to the four segment types. The weights are defined as  $\omega$  and  $\omega \in \{\omega_1, \omega_2, \omega_3, \omega_4\}$ ,  $\omega_t$  is the weight of the

$t$ th segment type. Normally,  $\omega_1 > \omega_3 > \omega_2 > \omega_4$ . Then, the weighted membership  $\rho$  of a segment can be expressed as:

$$\rho = \omega_i \times \mu(\bar{D^i}, e_i) \quad (20)$$

where  $\mu(\bar{D^i}, e_i)$  is the calculated membership of the  $i$ th segment by the multidimensional MFs,  $\bar{D^i}$  is the averaged prediction error and  $e_i$  is the environment condition.

4) *Membership assembling*: After the weighted membership calculation, each segment has its own weighted membership. However, only one membership is required as the input of FIS. Therefore, the multiple membership are assembled:

$$\hat{\mu} = \frac{\sum_{i=1}^n \omega_i \times l_i \times \mu(\bar{D^i}, e_i)}{\sum_{i=1}^n \omega_i \times l_i} \quad (21)$$

where  $l_i$  is the length of the  $i$ th segment,  $n$  is the segment number and  $\hat{\mu}$  is the result of the assembled membership.

### C. FIS Using Assembled Multidimensional MFs

In this subsection, FIS is improved and applied to calculating the output and detecting anomalies by the assembled multidimensional MFs.

Generally, in the process of fuzzy inference, firing level  $Fl$  is first calculated by the antecedent set and the input set:

$$Fl = Sup [\mu_g^1(x_1) \star \hat{\mu}_{F_1}(x_1)] \star Sup [\mu_g^2(x_2) \star \hat{\mu}_{F_2}(x_2)] \star \dots \star Sup [\mu_g^p(x_p) \star \hat{\mu}_{F_p}(x_p)] \quad (22)$$

where  $\star$  is the minimum t-norm operator [36],  $p$  is the number of inputs,  $\hat{\mu}_{F_i}(x_i)$  is the  $i$ th antecedent membership obtained by (21) and  $\mu_g^i(x_i)$  is the  $i$ th input membership. Since the proposed method belongs to singleton FIS, the membership of input set  $\mu_g$  can be regarded as constant “1”:

$$\forall \mu_g^i(x_i) = 1, \quad i = 1, 2, \dots, p \quad (23)$$

So,  $Fl$  can be simply expressed as:

$$Fl = \hat{\mu}_{F_1 \times F_2 \dots \times F_q}(x_1, x_2, \dots, x_p) = \hat{\mu}_{F_1}(x_1) \star \hat{\mu}_{F_2}(x_2) \star \dots \star \hat{\mu}_{F_q}(x_p) \quad (24)$$

Then, the fuzzy output set  $\mu_B(\delta)$  can be obtained by (25).

$$\mu_B(\delta) = \mu_G(\delta) \star Fl \quad (25)$$

where  $\mu_G(\delta)$  is the consequent MF. After that, all the output sets in the same linguistic variable but different rules are integrated by (26).

$$\mu_{\hat{B}}(\delta) = \mu_{B^1}(\delta) \oplus \mu_{B^2}(\delta) \oplus \dots \oplus \mu_{B^n}(\delta) \quad (26)$$

where  $\oplus$  is the maximum operator. Finally, the crisp output can be obtained by getting the gravity center of  $\mu_{\hat{B}}(\delta)$  and the anomaly can be detected the same as [29].

### D. The New CM Architecture of WTs

To sum up, Fig. 8 shows the new CM architecture of WTs by the proposed method. (1) Data prediction: The same as the conventional process in Fig. 1, the monitored data are predicted and prediction errors are obtained. (2) Fuzzification: Multidimensional MFs are established using the off-line prediction errors and their environment data (refer to

Section III.A). Then, online prediction errors are divided into segments and the calculated weighted memberships by the multidimensional MFs are assembled (refer to Section III.B). (3) Fuzzy inference and anomaly detection: FIS is finally improved and applied in CM of WTs (refer to Section III.C) by the assembled multidimensional MFs.

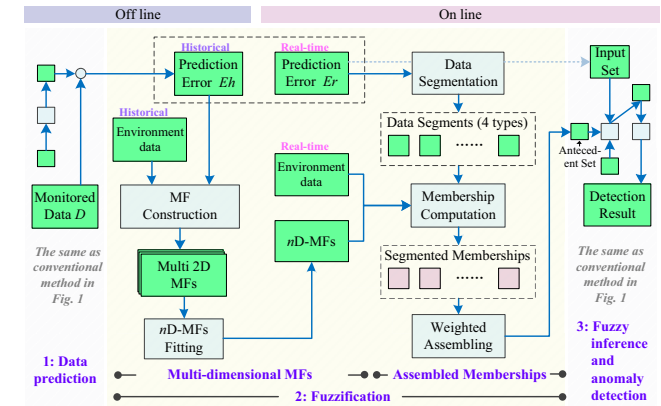


Fig. 8. The new CM architecture of WTs by the proposed method.

## IV. EXPERIMENTS AND DISCUSSIONS

### A. Experiment Settings

In this section, four groups of experiments are conducted to evaluate the proposed method. The experiment data are collected from a wind farm (WF) in the north of China. There are 33 WTs in the WF, and the SCADA data collected at an interval of 10 minutes are used in experiments. Fig. 9 shows pictures of the WF and the controlling center.

First, preprocessing has been conducted to remove the invalid data and impute the missing data. Then, only the data between the cut-in and cut-out wind speed are used. The widely-used back propagation neural network method [32] is applied to predicting the monitored data. One of the effective method [28] (2D-MF method for short) in the latest two-dimensional MFs studies [26]–[30] is compared with the proposed method in the following experiments.



Fig. 9. Pictures of the wind farm and the controlling center. (a) Wind farm. (b) Controlling center.

The parameter  $\gamma$  is set as 18 in experiments out of the following considerations. First, the value of  $\gamma$  should be set large enough to eliminate sudden data fluctuations. According to the conditions of the wind farm and the opinions of experts, the data of three to six hours as one segment ( $\gamma$  within the range of 18 to 36) is suitable. Second, the value of  $\gamma$  should be

set small to effectively follow WT data changes and achieve a better assembled CM effect. Therefore,  $\gamma$  is set as 18 (three hours with 18 data points) in experiments.

The parameter  $\omega$  are set as  $\omega_1 = 1.2$ ,  $\omega_2 = 0.9$ ,  $\omega_3 = 1.0$  and  $\omega_4 = 0.8$ . The values are determined by statistic method. First, the accuracies of data prediction for one day are computed, with segment type 1, 2, 3, 4 respectively, and the results are marked as  $A_1$ ,  $A_2$ ,  $A_3$  and  $A_4$ . Then, their averaged accuracies for 300 days are calculated and the results are marked as  $\overline{A}_1$ ,  $\overline{A}_2$ ,  $\overline{A}_3$  and  $\overline{A}_4$ . Therefore, the segment type weights  $\omega_1 : \omega_2 : \omega_3 : \omega_4 = \overline{A}_1 : \overline{A}_2 : \overline{A}_3 : \overline{A}_4$ , and suppose  $\omega_3 = 1.0$ , the values of  $\omega_1$ ,  $\omega_2$  and  $\omega_4$  can be determined.

Experiments are organized as follows: Experiment 1 is conducted to evaluate the proposed method in detecting early WT anomalies. Experiment 2 and Experiment 3 are carried out to verify the effectiveness of the proposed method in reducing missing detections and false alarms. Experiment 4 uses continuous data collected in a long period of time to further verify the effectiveness of the proposed method.

### B. Experiment 1

This experiment is carried out to evaluate the proposed method in detecting early WT anomalies. In early March 2015, the measured wind speed values were higher than normal due to the sensor fault of WT 16. The monitored data and the predicted data from March 17th to March 23th are shown in Fig. 10 (a) and their corresponding prediction errors are shown in Fig. 10 (b). The data curves indicate that the prediction errors gradually increase.

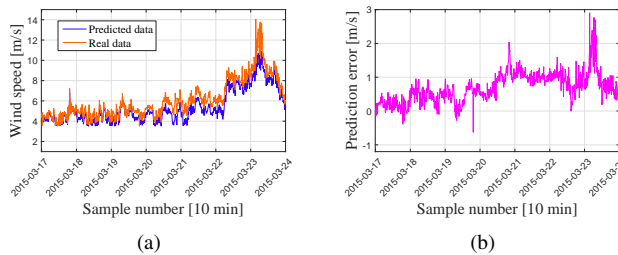


Fig. 10. The data of Experiment 1. (a) The real data and the predicted data of wind speed. (b) The prediction error.

The 2D-MF method and the proposed method ( $n$ D-CMF) are applied separately to detecting this anomaly. Fig. 11 shows the calculated MFs of the two methods. It can be found that compared with the conventional 2D-MFs, the proposed multidimensional MFs contain more detailed information and the extra environment dimension provides the membership distribution in different environment conditions, which would help to achieve more accurate CM results.

Then, prediction errors are processed by MFs. The 2D-MF method adopts the daily averaged data, whereas the proposed method uses data segments. Fig. 12 shows the data segments divided by the proposed method. It can be found that the prediction errors are properly divided into small segments and different weights are assigned in accordance with their segment types, which will help to monitor the conditions more accurately and make a better use of the effective data for CM.

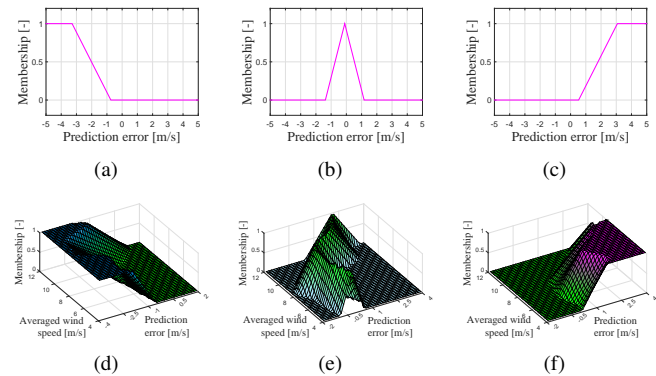


Fig. 11. MFs of the 2D-MF method: (a) low. (b) normal. (c) high. MFs of the proposed method: (d) low. (e) normal. (f) high.

Finally, using the fuzzy inference engine, the anomaly is detected by the two methods. Table I shows the anomaly detection results and Fig. 13 shows the detection details.

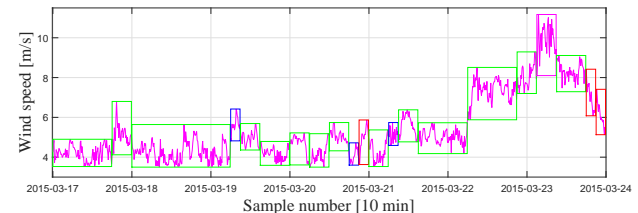


Fig. 12. Data segments divided by the proposed method in Experiment 1.

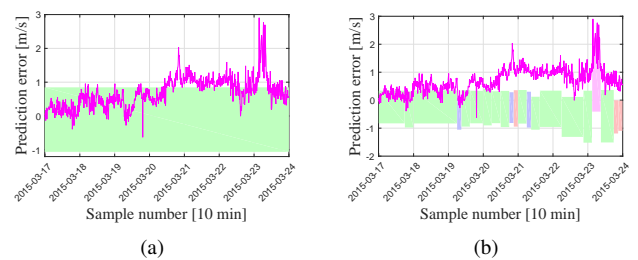


Fig. 13. Results of Experiment 1. The colored region is normal area judged by the methods. (a) The 2D-MF method. (b) The proposed method.

The results show that the proposed method detects the anomaly two days earlier than the 2D-MF method. Fig. 13 shows that: (1) When using the 2D-MF method, the calculated normal range forms two fixed boundaries (the upper bound and the lower bound) due to the limitation of 2D-MFs. The boundaries reflect the normal range of the averaged environment conditions. The 2D-MF method did not detect the early anomaly until March 20th. (2) When using the proposed method, the upper bound and the lower bound fluctuate with different environments, making the CM more flexible and sensitive to slight anomalies.

On March 18th and March 19th, the prediction errors were within the normal range of the 2D-MF method, whereas they exceed the upper bound of proposed method. The advantage of the proposed method may attribute to the using of the assembled multidimensional MFs, which include the environment

TABLE I  
EXPERIMENT RESULTS OF EXPERIMENT 1.

Method	The date in March 2015						
	17	18	19	20	21	22	23
2D-MF	N	N	N	A	A	A	A
proposed	N	A	A	A	A	A	A

“N” denotes normal and “A” denotes anomaly.

factor. It makes the CM more flexible and adaptable. It can be concluded that the proposed method can detect early anomalies more effectively.

### C. Experiment 2

This experiment is carried out to verify the effectiveness of the proposed method in reducing missing detections of anomalies. On July 29th, 2016, in the process of software updating, some parameters were set incorrectly. As a result, the measured wind speed values were a little higher than the actual values. A few days later, the fault was corrected. According to the experiences of experts, the rule of detecting such kind of fault can be expressed as: “IF (wind speed == high) AND (active power == normal) AND (pitch angle == normal) THEN (diagnosis: wind speed measured too high)”. Fig. 14 (a) shows the monitored and the predicted data of wind speed. Fig. 14 (b) shows their corresponding prediction errors.

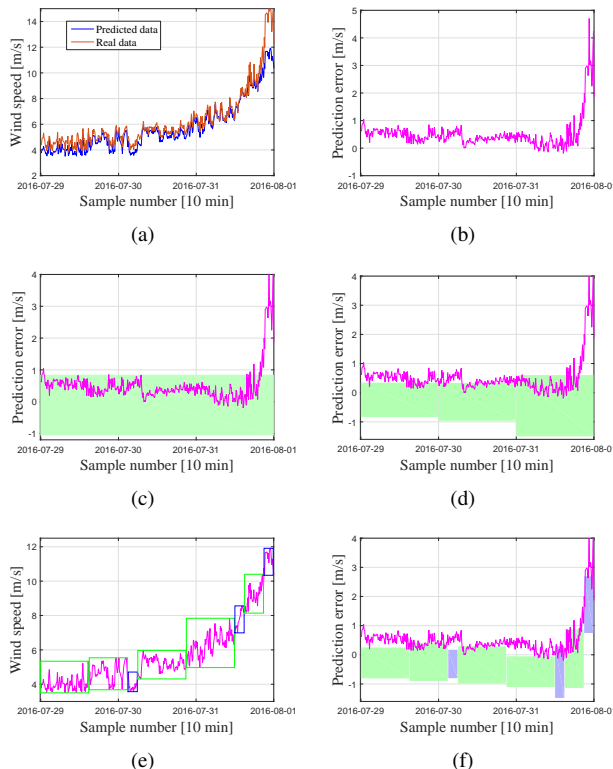


Fig. 14. Results of Experiment 2. (a) The real data and the predicted data. (b) Prediction error. (c) Results of 2D-MF method. (d) Results of  $n$ D-MF method. (e) Segments of  $n$ D-CMF method. (f) Results of  $n$ D-CMF method.

Three methods are applied in this experiment to make better comparisons: the 2D-MF method (such as the method used in

[28] and [29]), the proposed method without the assembled memberships ( $n$ D-MF method) and the proposed method with the assembled memberships ( $n$ D-CMF method). Experiment results are shown in Table II and detection details are shown in Fig. 14 (c), (d) and (f).

TABLE II  
EXPERIMENT RESULTS OF EXPERIMENT 2.

Method	07-29	07-30	07-31
2D-MF	N (0.04)	N (0.00)	N (0.21)
$n$ D-MF	A (0.85)	A (0.73)	N (0.46)
$n$ D-CMF	A (0.89)	A (0.77)	A (0.59)

“N” denotes normal and “A” denotes anomaly.

The experiment results show that: (1) When using 2D-MF method, most of the prediction errors are within the normal range. On July 31th, although some data exceeded the upper bound, the averaged value remained within the normal range. So all the conditions of the three days are judged as normal. (2) When using  $n$ D-MF method, the multidimensional MFs are applied, and most of the prediction errors exceed the normal range. The conditions of the first two days are detected as anomalies. However, on July 31th, the obtained result shows that the condition on this day is misjudged as normal. (3) When using  $n$ D-CMF method, both the multidimensional MFs and the assembled memberships are applied. Fig. 14 (e) shows the divided segments. It can be found that the normal range changes in different environments. Meanwhile, different types of segments are identified as shown in different colors in Fig. 14 (f) and different membership weights are all assigned. That makes the CM more flexible. Finally, the conditions of all the three days are judged as anomalies. It can be concluded that the proposed method can reduce the missing detection of anomalies more effectively.

### D. Experiment 3

This experiment is conducted to evaluate the proposed method in reducing false alarms. The settings of this experiment are the same as those in Experiment 2 and all the three methods are applied in this experiment. The normal data of four days in March, 2016 are used. Fig. 15 and Table III show the detailed data and experiment results.

TABLE III  
EXPERIMENT RESULTS OF EXPERIMENT 3.

Method	03-21	03-22	03-23	03-24
2D-MF	N (0.00)	A (0.56)	N (0.44)	N (0.00)
$n$ D-MF	N (0.00)	N (0.01)	N (0.01)	N (0.00)
$n$ D-CMF	N (0.00)	N (0.00)	N (0.00)	N (0.00)

“N” denotes normal and “A” denotes anomaly.

The wind speed is relatively high in these four days. (1) When using 2D-MF method, many prediction errors exceed the upper bound. As a result, the condition on March 22th is judged as an anomaly, which is a false alarm. (2) When using

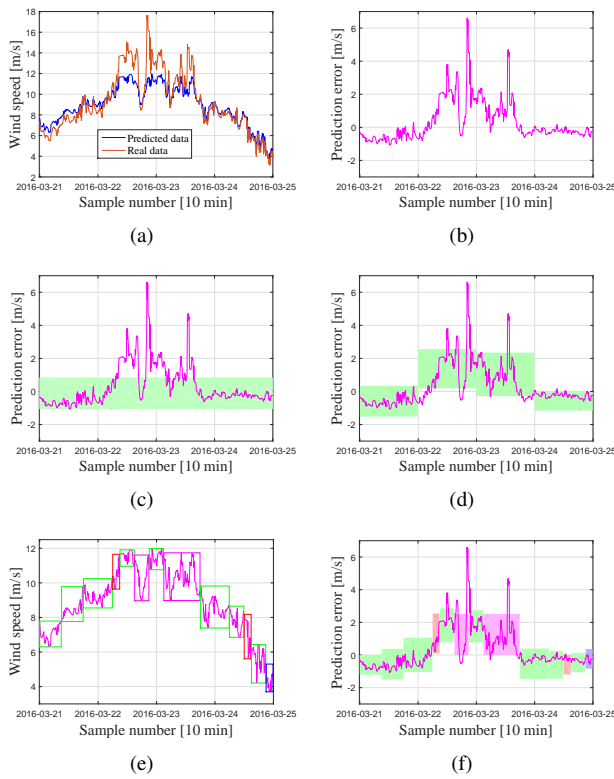


Fig. 15. Results of Experiment 3. (a) The real data and the predicted data. (b) Prediction error. (c) Results of 2D-MF method. (d) Results of  $n$ D-MF method. (e) Segments of  $n$ D-CMF method. (f) Results of  $n$ D-CMF method.

$n$ D-CMF method and  $n$ D-CMF method, multidimensional MFs are used and the normal range changed with different environments. In  $n$ D-CMF method, assembled memberships are also applied. The conditions in the three days are all judged as normal and no false alarms are given. It can be concluded that the proposed method can reduce the false alarms more effectively.

#### E. Experiment 4

In this experiment, more data (data of each WT for 150 consecutive days) are used to further evaluate the proposed method. The experiment settings are the same as those in Experiment 2 and 3. Three WTs with the same anomaly are used to do the evaluation. Table IV shows the experiment settings and results. It can be found: (1) 2D-MF method detects anomalies in 6 out of 9 days and misjudged the normal conditions in two days as anomalies. (2)  $n$ D-MF method detects anomalies in 8 out of 9 days and no false alarms are given. (3)  $n$ D-CMF method detects all the anomalies and no false alarms are given. It can be concluded that the proposed method is effective in CM and anomaly detection.

#### F. Discussion

In this subsection, the advantages and deficiencies of the proposed method are summarized.

The advantages of the proposed method can be summarized as: (1) Detecting early anomalies. The proposed multidimensional MF in this paper can deal with the environment factor so

TABLE IV  
EXPERIMENT RESULTS OF EXPERIMENT 4.

Method	Total Days	Anomaly Days	Right Detections	False Alarms
2D-MF	450	9	6 / 9	2
$n$ D-MF	450	9	8 / 9	0
$n$ D-CMF	450	9	9 / 9	0

that the early anomalies can be detected. (2) Reducing missing detections and false alarms. The proposed multidimensional MF and the assembled membership in this paper can precisely process the changeable data, so that the missing detections and false alarms can be reduced.

For the proposed multidimensional MF generation method, it is a workable and effective alternative to the method of obtaining multidimensional MF by directly fitting the collected data. In practice, the method of directly fitting the collected data does not work because the data, especially the anomaly data that could cover most of the conditions are insufficient. The proposed method obtains 3D MF by fitting all the 2D MFs, which requires less data and is more effective.

For the proposed assembled membership, it can enhance the positive effect of high quality data and reduce the negative effect of poor quality data. Unlike the physical model method, which is difficult to build, the assembled membership is obtained by data-driven method, which would be robust and easier to be implemented.

The deficiencies of the proposed method mainly include: (1) More off-line preparations. To apply the proposed method, more 2D MFs should be established and a fitting method should be applied. (2) More online computations. In online computation, the environment variables should be also considered. And the data should be separated into data segments to be further processed.

## V. CONCLUSION

This paper proposes a new CM approach of WTs based on assembled multidimensional MFs using FIS, with the aim of reducing the negative effect on CM from changeable environments. Multidimensional MFs are firstly proposed by fitting different environment conditions, so that the environment factor is fused into MFs. Then, the data segmentation method is applied to dividing the input data in accordance with data features. Also, the divided segments are classified into four types with different membership weights. Then, the calculated memberships of all the segments are assembled for fuzzy inference. Based on the assembled multidimensional MFs, a new architecture of CM is established. Four groups of experiments are conducted to prove the effectiveness of the proposed method in reducing the negative effect of changeable environments on CM.

## ACKNOWLEDGMENT

This work was supported in part by the Fundamental Research Funds for the Central Universities of China

(N170404019), the National Natural Science Foundation of China (61973071, 61627809), and the Liaoning Natural Science Foundation of China (2019-KF-03-04).

## REFERENCES

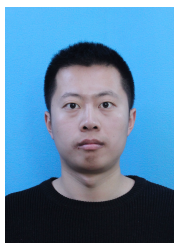
- [1] T. K. Mahmoud, Z. Y. Dong, and J. Ma, "A developed integrated scheme based approach for wind turbine intelligent control," *IEEE Transactions on Sustainable Energy*, vol. 8, no. 3, pp. 927–937, 2017.
- [2] P. Qian, D. Zhang, X. Tian, Y. Si, and L. Li, "A novel wind turbine condition monitoring method based on cloud computing," *Renewable energy*, vol. 135, pp. 390–398, 2019.
- [3] W. Qiao and D. Lu, "A survey on wind turbine condition monitoring and fault diagnosis/part i: Components and subsystems," *IEEE Transactions on Industrial Electronics*, vol. 62, no. 10, pp. 6536–6545, 2015.
- [4] J. Helsen, C. Devriendt, W. Weijtjens, and P. Guillaume, "Condition monitoring by means of scada analysis," in *Proceedings of European Wind Energy Association International Conference Paris*, 2015.
- [5] P. Qian, X. Ma, D. Zhang, and J. Wang, "Data-driven condition monitoring approaches to improving power output of wind turbines," *IEEE Transactions on Industrial Electronics*, vol. 66, no. 8, pp. 6012–6020, 2018.
- [6] J. Wang, W. Qiao, and L. Qu, "Wind turbine bearing fault diagnosis based on sparse representation of condition monitoring signals," *IEEE Transactions on Industry Applications*, vol. 55, no. 2, pp. 1844–1852, 2018.
- [7] L. Zhang, Z.-Q. Lang, and M. Papaelias, "Generalized transmissibility damage indicator with application to wind turbine component condition monitoring," *IEEE Transactions on Industrial Electronics*, vol. 63, no. 10, pp. 6347–6359, 2016.
- [8] H. Shao, Z. Gao, X. Liu, and K. Busawon, "Parameter-varying modelling and fault reconstruction for wind turbine systems," *Renewable Energy*, vol. 116, pp. 145–152, 2018.
- [9] J. P. Salameh, S. Cauet, E. Etien, A. Sakout, and L. Rambault, "Gearbox condition monitoring in wind turbines: A review," *Mechanical Systems and Signal Processing*, vol. 111, pp. 251–264, 2018.
- [10] B. Yang, R. Liu, and X. Chen, "Fault diagnosis for a wind turbine generator bearing via sparse representation and shift-invariant k-svd," *IEEE Transactions on Industrial Informatics*, vol. 13, no. 3, pp. 1321–1331, 2017.
- [11] Y. Zhang, W. Lu, and F. Chu, "Planet gear fault localization for wind turbine gearbox using acoustic emission signals," *Renewable Energy*, vol. 109, pp. 449–460, 2017.
- [12] J. Zhu, J. M. Yoon, D. He, and E. Bechhoefer, "Online particle-contaminated lubrication oil condition monitoring and remaining useful life prediction for wind turbines," *Wind Energy*, vol. 18, no. 6, pp. 1131–1149, 2015.
- [13] E. Alizadeh, N. Meskin, and K. Khorasani, "A dendritic cell immune system inspired scheme for sensor fault detection and isolation of wind turbines," *IEEE Transactions on Industrial Informatics*, vol. 14, no. 2, pp. 545–555, 2018.
- [14] R. Rahimilarki, Z. Gao, A. Zhang, and R. J. Binns, "Robust neural network fault estimation approach for nonlinear dynamic systems with applications to wind turbine systems," *IEEE Transactions on Industrial Informatics*, 2019.
- [15] R. A. A. Habeeb, F. Nasaruddin, A. Gani, I. A. T. Hashem, E. Ahmed, and M. Imran, "Real-time big data processing for anomaly detection: A survey," *International Journal of Information Management*, vol. 45, pp. 289–307, 2019.
- [16] Y. Wang, X. Ma, and P. Qian, "Wind turbine fault detection and identification through pca-based optimal variable selection," *IEEE Transactions on Sustainable Energy*, vol. 9, no. 4, pp. 1627–1635, 2018.
- [17] P. B. Dao, W. J. Staszewski, T. Barszcz, and T. Uhl, "Condition monitoring and fault detection in wind turbines based on cointegration analysis of scada data," *Renewable Energy*, vol. 116, pp. 107–122, 2018.
- [18] K.-Y. Oh, J.-Y. Park, J.-S. Lee, B. I. Epureanu, and J.-K. Lee, "A novel method and its field tests for monitoring and diagnosing blade health for wind turbines," *IEEE Transactions on Instrumentation and Measurement*, vol. 64, no. 6, pp. 1726–1733, 2015.
- [19] A. Stetco, F. Dinnmohammadi, X. Zhao, V. Robu, D. Flynn, M. Barnes, J. Keane, and G. Nenadic, "Machine learning methods for wind turbine condition monitoring: A review," *Renewable Energy*, vol. 133, pp. 620–635, 2019.
- [20] G. Jiang, H. He, J. Yan, and P. Xie, "Multiscale convolutional neural networks for fault diagnosis of wind turbine gearbox," *IEEE Transactions on Industrial Electronics*, vol. 66, no. 4, pp. 3196–3207, 2019.
- [21] L. Wang and Z. Zhang, "Automatic detection of wind turbine blade surface cracks based on uav-taken images," *IEEE Transactions on Industrial Electronics*, vol. 64, no. 9, pp. 7293–7303, 2017.
- [22] L. Wang, Z. Zhang, H. Long, J. Xu, and R. Liu, "Wind turbine gearbox failure identification with deep neural networks," *IEEE Transactions on Industrial Informatics*, vol. 13, no. 3, pp. 1360–1368, 2017.
- [23] P. Guo, D. Infield, and X. Yang, "Wind turbine generator condition-monitoring using temperature trend analysis," *IEEE Transactions on Sustainable Energy*, vol. 3, no. 1, pp. 124–133, 2012.
- [24] M. Kumar, Y. Mao, Y. Wang, T. Qiu, Y. Chenggen, and W. Zhang, "Fuzzy theoretic approach to signals and systems: static systems," *Information Sciences*, vol. 418, pp. 668–702, 2017.
- [25] S. Simani, S. Farsoni, and P. Castaldi, "Fault diagnosis of a wind turbine benchmark via identified fuzzy models," *IEEE Transactions on Industrial Electronics*, vol. 62, no. 6, pp. 3775–3782, 2015.
- [26] J. Liu, F. Qu, X. Hong, and H. Zhang, "A small-sample wind turbine fault detection method with synthetic fault data using generative adversarial nets," *IEEE Transactions on Industrial Informatics*, vol. 15, no. 7, pp. 3877–3888, 2019.
- [27] H. Li, Y. Hu, C. Yang, Z. Chen, H. Ji, and B. Zhao, "An improved fuzzy synthetic condition assessment of a wind turbine generator system," *International Journal of Electrical Power & Energy Systems*, vol. 45, no. 1, pp. 468–476, 2013.
- [28] P. Sun, J. Li, C. Wang, and X. Lei, "A generalized model for wind turbine anomaly identification based on scada data," *Applied Energy*, vol. 168, pp. 550–567, 2016.
- [29] M. Schlechtingen, I. F. Santos, and S. Achiche, "Wind turbine condition monitoring based on scada data using normal behavior models. part 1: System description," *Applied Soft Computing*, vol. 13, no. 1, pp. 259–270, 2013.
- [30] M. Schlechtingen and I. F. Santos, "Wind turbine condition monitoring based on scada data using normal behavior models. part 2: Application examples," *Applied Soft Computing*, vol. 14, pp. 447–460, 2014.
- [31] W. Yang, Z. Lang, and W. Tian, "Condition monitoring and damage location of wind turbine blades by frequency response transmissibility analysis," *IEEE Transactions on Industrial Electronics*, vol. 62, no. 10, pp. 6558–6564, 2015.
- [32] W. Qiao and D. Lu, "A survey on wind turbine condition monitoring and fault diagnosis/part ii: Signals and signal processing methods," *IEEE Transactions on Industrial Electronics*, vol. 62, no. 10, pp. 6546–6557, 2015.
- [33] A. Alzahrani, P. Shamsi, C. Dagli, and M. Ferdowsi, "Solar irradiance forecasting using deep neural networks," *Procedia Computer Science*, vol. 114, pp. 304–313, 2017.
- [34] K. Wang, H. Li, Y. Feng, and G. Tian, "Big data analytics for system stability evaluation strategy in the energy internet," *IEEE Transactions on Industrial Informatics*, vol. 13, no. 4, pp. 1969–1978, 2017.
- [35] A. Stuikys and J. K. Sykulski, "An efficient design optimization framework for nonlinear switched reluctance machines," *IEEE Transactions on Industry Applications*, vol. 53, no. 3, pp. 1985–1993, 2017.
- [36] J. M. Mendel, *Uncertain rule-based fuzzy systems*. Springer, 2017.



**Fuming Qu** (S'18) received B.S. degree and M.S. degree in electronic information engineering from Northeastern University, Shenyang, China, in 2006 and 2008 respectively. He is currently pursuing Ph.D. degree of power electronics and power transmission with the School of Information Science and Engineering, Northeastern University. His current research interests include condition monitoring and fault diagnosis of wind turbine, the application of data-driven methods in the field of industrial electronics.



**Jinhai Liu** (M'09) received the B.S. degree in automation from the Harbin Institute of Technology, Harbin, China, in 2002, the M.S. degree in power electronics and power transmission, and the Ph.D. degree in control theory and control engineering from Northeastern University, Shenyang, China, in 2005 and 2009, respectively. He is currently a professor and Doctoral supervisor with Northeastern University. His current research interests include data driven fault diagnosis, industrial big data analysis, and safety technology of long pipelines.



**Hongfei Zhu** received the B.S. degree in electrical engineering and automation from the Suihua University, Suihua, China, in 2015, the M.S. degree in power electronics and power transmission from Northeastern University, Shenyang, China, in 2019. He is currently pursuing Ph.D. degree of control science and engineering with the School of Information Science and Engineering, Northeastern University. His current research interests include Multi-agent system, fuzzy control, and fuzzy logic system.



**Dong Zang** received the B.S. degree in automation from the Hefei University, Hefei, China, in 2013, and the M.S. degree in control theory and control engineering from Liaoning Technical University, Huludao, China, in 2016. He is working toward the Ph.D. degree in control theory and control engineering from Northeastern University, Shenyang, China. His research interests include fault diagnosis, data mining and their industrial applications.